Journal Of Harmonized Research (JOHR)

Journal Of Harmonized Research in Applied Sciences
3(4), 2015, 283-300

ISSN 2321 – 7456

Original Research Article

COPPER COMPLEXES CHELATION AND ITS STRUCTURE AND PHOSPHORESCENCE

Rajeev Kumar, Shivadhar Sharma

Department of Chemistry, Magadh University, Bodh Gaya, Bihar 824234

Abstract: With the aim to obtain new phosphorescent Cu (I) compounds, several new 1, 2-phenyl-bridged P^N, P$_\wedge$N^P, and N^P^N chelate ligands were designed and synthesized. These ligands were found to form complexes with Cu (I) ion readily via either solution reactions or solid-state grinding process. The new Cu (I) compounds based on this class of ligands display phosphorescence with emission color ranging from blue to red. The structure of the ligand and the nature of the N-heterocycle in the chelate ligands were found to have a significant impact on the phosphorescent properties of the Cu (I) compounds.

INTRODUCTION

Cu(I) complexes have recently attracted great attention as promising luminescent materials, due to their low cost, interesting phosphorescent properties, diverse structural features, and potential applications in organic light-emitting diodes (OLEDs),[1-5] photosensitizers,[6-8] sensing devices,[9] biological imaging,[10] and dye-sensitized solar cells (DSCs).[11-13] A large number of mono- and polynuclear Cu(I) complexes have been developed and investigated for various applications.[14, 15]

For Correspondence:
Imrajeev_bio@yahoo.com.
Received on: October 2015
Accepted after revision: December 2015
Downloaded from: www.johronline.com

In particular, Cu(I) complexes that contain N-heteroaryl donors have been shown to be very promising as luminescent materials.[16, 17] Many examples of bright phosphorescent Cu(I)-halide complexes based on mono- or bidentate N-heteroaryl ligands with tunable emission colors have been demonstrated.[18]

Cu(I) complexes containing a p-methylpyridine ligand, [CuX(PPh_3)2(4-Mepy)] (X = Cl, Br, I), have been shown to be a highly promising blue TADF (thermally activated delayed fluorescence) emitter.[19] However, the poor stability of many of the previously reported Cu(I) complexes in solution greatly hinders their practical applications.[18,19] Combining the tunable electronic properties of N-heteroaryl ligands with the strong stabilizing ability of phosphine donors exerted on the Cu(I) center, the use of P^N chelate ligands has been shown to be an effective strategy in achieving stable and bright luminescent Cu(I) compounds, and many

luminescent Cu(I) complexes based on P^N, N^P^N, and P^N^P ligands were investigated.[20-26] However, as shown in Chart 1, the previously investigated systems focused mainly on the ligands with the phosphine unit being bound directly to an N-heteroaryl ring or an aliphatic group,[24, 27, 28] with the former being usually bridging or monochelate ligands due to the small chelate bite angle, whereas the latter are often not effective in achieving bright phosphorescent copper(I) compounds.[23,24] With the aim to open the scope of P^N chelate ligands and to examine the impact of new P^N chelate ligands on phosphorescent properties of copper(I) compounds, we designed and synthesized a series of 1,2-phenyl-bridged P^N, P^N^P, and N^P^N ligands shown in Chart 1 and investigated the binding modes of the new ligands with the copper(I) ion and the luminescent properties of the resulting copper(I) complexes. The details are presented herein.

Results and Discussion

Syntheses of Ligands and Copper Complexes. Ligand **L1** was prepared by a literature procedure.[29] The synthetic procedures for **L2**, **L3**, and **L4** are shown in Scheme 1. The precursor compounds 2-(2-fluorophenyl)pyridine [30] and 2,6- bis(2-fluorophenyl)pyridine[31] for **L2** and **L3** were prepared using literature procedures. Ligands **L2** and **L3** were obtained by the reaction of the corresponding fluorine-substituted precursor with KPPh2 in the presence of 18-crown-6 in 71 and 80% yield, respectively. In the case of ligand **L4**, the attachment of a 2-pyridylphenyl group to the phosphine center was accomplished by lithiation of 2-(2-bromophenyl) pyridine with n-butyl lithium, followed by the addition of $PPhCl_2$ in 57% yield. Ligands **L3** and **L4** were designed and synthesized with the aim to use them as tridentate chelate ligands to constrain the geometry of the Cu (I) center. To examine the impact of different structures and compositions on phosphorescene, for ligand **L1**, three different copper(I) complexes, a neutral monomer 1, a neutral dimer 2, and a cationic monomer 3, were synthesized using the procedure shown in Scheme 2 in 80−85% yield. For **L2**, attempts were made to prepare both the neutral monomer and the dimer, analogues of 1 and 2. However, only the monomer 4 was successfully isolated as a clean product in 90% yield. For ligand L3 and L4, the reaction with CuI in CH_2Cl_2 or THF led

to the formation of the corresponding Cu(I) complexes 5 and 6 in 80 and 90% yield, respectively.

Inspired by the recent work of Kato[32] and co-workers on efficient mechano chemical synthesis of Cu (I) complexes, we attempted the synthesis of the new Cu (I) complexes by the solid-state grinding process. Indeed, compounds 1, 2, and 4 can be obtained readily in high yield (the second yield in Scheme 2) by simply mixing and grinding the corresponding ligands with CuI in a mortar, as shown by the photographs in Figure 1, which supports the generality of Kato's procedure. Consistent with the observation reported by Kato and co-workers, the addition of a few drops of acetonitrile to aid the mixing of CuI with the ligand is necessary in order for the grinding process to work effectively.[32] The new Cu (I) complexes were fully characterized by NMR and elemental analyses. All new Cu (I) compounds have a poor solubility in solvents such as $CDCl_3$, except the cationic compound 3 and compound 5, which have a moderate solubility. Compounds 1 and 4 display two distinct 31P chemical shifts in 31P NMR spectra, consistent with the presence of a PPh3 donor and a PPh2 donor from the chelate ligand. Compound 5 displays a single peak at −6.79 ppm in the 31P NMR spectrum, indicating that both phosphorus atoms in the L3 ligand are bound to the Cu(I) center in a symmetric manner. NMR data indicated that compounds 1−6 are stable in solution. To fully establish the structures of the new Cu (I) compounds, single-crystal X-ray diffraction analyses were performed for all compounds.

Crystal Structures of the Copper Complexes. The crystal structures of the six new Cu(I) complexes are shown in Figures 2−4, respectively. Important bond lengths and angles are provided in Table 1.

Solvent molecules such as $CHCl_3$, CH_2Cl_2, or THF were found in the crystal lattices of all complexes, except that of compound 3. The geometry around the Cu (I) center in all compounds, except in 5, is a distorted tetrahedron. Ligand **L1** chelates to the Cu atom, forming a twisted six-membered chelate ring in compounds 1−3. The bite angles of **L1** in 1-3 are similar (88.54(7), 86.04(4), and 86.38(7) °, respectively), despite the different coordination environment around the Cu center in these complexes. For L1- based complexes, the Cu−I and the Cu−P bond lengths in dimer 2 are somewhat shorter than those in monomer 1 due to the reduced steric congestion in the dimer. The Cu(1)−Cu(1′) separation distance in 2 is 2.7989(5) Å, similar to the sum of the van der Waals radius of copper (2.80 Å), thus excluding any significant metallophilic interactions. The cationic complex 3 also displays Cu−P and Cu−N bond lengths shorter than those of 1, which may be attributed to the positive charge of the Cu (I) atom that enhances ligand binding affinity. The crystal data established that the triazolyl-based ligand L2 is an effective bidentate chelate ligand for binding to the Cu (I) ion as its pyridyl analogue **L1** does. Ligand L2 forms a monomer complex 4, which is an analogue of compound 1 with a similar coordination environment. The chelate bite angle (89.8(1)°) of L2 in 4 is similar to that of **L1** in 1. The Cu−N bong length in 4 (2.076(3) Å) is, however, significantly shorter than that in 1 (2.155(2) Å). The pyridyl−phenyl unit in 1 is much more twisted than the triazolyl−phenyl unit in 4, as evidenced by the much larger dihedral angle in 1 (42.1°), relative to that in 4 (29.5°). As a consequence, the six-membered chelate ring in 4 is much less puckered than that in 1. In the crystal lattice, compound 1 displays intermolecular π-stacking interactions between the phenyl rings of L1 ligands (see Figure S2), while in contrast, similar π-stacking interactions were not observed for 4 (see Figure S3).

Although both compounds 5 and 6 contain tridentate chelate ligand, their structures are very different. For 5, the tridentate ligand L3 is bound to the Cu(I) center via the two phosphorus atoms only, which along with the iodo ligand result in a trigonal planar geometry around the Cu(I) center, as indicated by the sum of the three bond angles around the Cu center (360°). The pyridyl ring is approximately parallel to one adjacent phenyl ring and perpendicular to the other phenyl ring. The pyridyl N (1) atom in 5 is 2.626(1) Å away from the Cu atom, with the pyridyl ring being approximately parallel to the CuP_2I plane, thus ruling out any significant σ binding interactions with the Cu center. The pyridyl ring in 5 may have only very weak π interaction with the Cu ion. Although three coordinate Cu(I) compounds are much less common than four-coordinate ones, similar three-coordinate Cu(I) compounds that display a weak π binding interaction between a Cu(I) ion and an internal aryl ring have been reported previously.[24, 33] For 6, the L4 ligand is bound to the Cu(I) center through both nitrogen atoms and the phosphorus atom. The two P^N bite angles in 6 (90.27(9) and 96.79(9)°) are greater than that in 1. The Cu(1)−P(1) bond length (2.183(1) Å) in 6 is the shortest among the six Cu(I) compounds, which may be attributed to the greater steric constraint in 6. Ligand **L4** in 6 is twisted to match the coordination geometry of Cu (I) ion, with the dihedral angles between the pyridyl and the adjacent phenyl rings being 42.0 and 49.3°, respectively. The crystal structural data established that ligand **L3** is not an effective tridentate chelate ligand for Cu(I) due to the relatively rigid and π-conjugated backbone of this ligand, whereas the flexibility provided by ligand **L4** makes it possible to bind to the Cu(I) ion as a tridentate ligand. Crystal data also revealed the presence of extensive π-stacking interactions between pyridyl rings and between pyridyl and phenyl rings in the crystal lattice of compound 6, similar to that observed for compound 1 (see Figure S4).

Absorption Spectra of the Copper Complexes. All copper(I) compounds reported here have a yellow or light yellow color in solution and the solid state, except compounds 4 and 5, which are colorless. The absorption spectra of the Cu (I) complexes 1−6 recorded in CH_2Cl_2 are shown in Figure 5, and the data

are given in Table S1. Compared with the absorption spectra of the free ligands **L1**, **L2**, **L3**, and **L4** in CH_2Cl_2 (see Figure S5), the intense absorption bands between 260 and 310 nm ($\varepsilon > 20\ 000\ M^{-1}\ cm^{-1}$) can be assigned to ligand-centered (LC) π−π* transition. The shoulder peak at ∼310−350 nm can be assigned to the π−π* transition within the N-heterocycle moiety. The broad and very weak low-energy tails at ∼350−400 nm, which are not observed in the corresponding free ligand spectrum, may be ascribed to the charge transfer transition involving the copper ion or the iodide ligand and are believed to be responsible for the observed pale yellow or yellow color for some of the copper compounds. To further understand the electronic properties of the copper(I) compounds, time-dependent density functional theory (TD-DFT) computational study was performed for all complexes based on the optimized ground-state geometries. The details of the TD-DFT data are given in Tables S2−S9. As shown in Figure 6, for iodo-containing complexes 1, 2, and 4−6, the HOMO has a large contribution from the iodo ligand and significant contribution from the Cu(I), whereas for the cationic complex 3, the HOMO resides mainly on the Cu(I) and Cu−P σ bonds. The LUMO is mainly located on the Nheterocycle and the adjacent phenyl ring for all complexes. For all compounds except the cationic molecule 3, the vertical excitations to S1 and S2 states involve charge transfer transitions from the iodide lone pair electrons to the π* orbital of the pyridyl−phenyl unit of the chelate ligand with low oscillator strengths (<0.01). For compound 3, the vertical excitations to S1 and S2 involve mainly σ (Cu−P bonds) to the π* orbital of the pyridyl−phenyl unit of the chelate ligand with a low oscillator strength. The transitions to the higher excited state do show appreciable oscillator strengths. For example, for compound 1, the S0 → S3 transition has an oscillator strength of 0.0141 (HOMO−2 → LUMO, 99%), whereas for 4, the S0 → S4 transition has an oscillator strength of 0.0111 (HOMO−2 → LUMO, 95%). Both of these transitions can be described as σ (Cu−I bond) to π* (the P∧N chelate ligand) transitions. The S0 → T1 transitions for all complexes involve mainly the HOMO → LUMO transition. DFT data indicate that the vertical excitation energy to S1 and T1 for 4 is about 0.2 eV higher than that of the analogue 1. Interestingly, DFT data revealed that the difference between the S1 and T1 energies for complexes 1, 4, and 5 is very small (0.02, 0.03, and 0.01 eV, respectively). Based on the DFT data, the low-energy absorption tail of the copper complexes can be attributed to MLCT/iodide-to-ligand charge transfer for the iodo-containing complexes 1, 2, and 4−6 and MLCT/σ to π* transition for complex 3.

Phosphorescence of the Copper Complexes. Compounds 1−6 are either non-emissive or weakly emissive in solution at ambient temperature. However, these compounds are all emissive in the solid state at ambient temperature with distinct emission colors ranging from green−blue to red and contrasting brightness, as shown by the photograph in Figure 7. Therefore, the investigation on phosphorescent properties of this class of compounds was focused on the samples in the solid state, doped poly(methyl methacrylate) (PMMA) films or in a frozen glass (2-Me-THF, 77 K). The emission spectra of compounds 1−6 as powders and crystals at 298 K are shown in Figure 8, and those of the doped PMMA films (5%) at 298 K and the frozen solutions in 2-Me-THF at 77 K are shown in Figure 9. All of the emission spectra for this class of compounds are broad and unstructured, indicating that the emissions are likely from charge transfer transitions, [34, 35] which appear to agree with the TD-DFT data. The decay lifetimes of the copper compounds are in the 5−177 μs range, consistent with phosphorescence. The decay lifetimes at 77 K for all compounds are much longer than those recorded at ambient temperature due to the greatly reduced vibrational quenching/ structural relaxation at low temperature.

As a neat solid, all six compounds display phosphorescence at ambient temperature. For the three L1-based complexes 1, 2, and 3, the emission wavelength varies significantly with λ_{max} = 601, 649, and 616 nm, respectively. The significant red shift of the dimer complex 2 compared to the monomer 1 is consistent with that in the previous report on related compounds.35 The decay lifetimes of these three compounds are similar, 8.3−9.0 μs. Significantly, however, only compound 1 has moderate emission quantum efficiency (0.15), whereas 2 and 3 emit weakly. These data illustrate that the ligands and the environment about the Cu(I) center have a dramatic impact on both emission energy and efficiency. As crystals, the emission energy of compounds 1−3 follows a trend similar to that of the powder sample, although the λmax of 1 and 2 experiences a 20 nm blue shift, which may be attributed to the presence of CHCl3 solvent molecules in the crystal lattice that reduces intramolecular interactions. The emission quantum yield of 1 is more than doubled (0.33) in the crystalline state than that in the powder state. In 5% doped PMMA films, the emission spectra of 2 and 3 experiences a significant blue shift, which may be attributed to reduced intermolecular interaction due to dilution, compared to neat powders or crystals. The emission energy of the PMMA film of compound 1 does not change significantly from its powder state; however, its emission efficiency decreases drastically from 0.15 to 0.02, due to the great increase of nonradiative decay rate constant (knr; see Table 2), caused perhaps by the reduced structural rigidity in PMMA. In the frozen solution at 77 K, the emission efficiency of 1 becomes impressive, reaching 0.38, which supports that emission quenching via vibrational or structural distortion is a main cause for its low emission efficiency at ambient temperature. For 2 and 3, the emission efficiency of the frozen solution at 77 K is still very low. Thus, the low emission quantum efficiency of 2 and 3 is the intrinsic nature of these two molecules. The dimer and the cationic structures are therefore undesirable for achieving bright Cu(I) phosphorescent compounds based on the 1,2-phenyl-bridged P^N chelate ligands. For this reason, our investigation on L2-based complexes focused on the monomer compound 4 only.

As an analogue of compound 1, compound 4 has extremely high emission quantum efficiency (0.97) in the frozen solution at 77 K. Its emission efficiency as a neat powder at ambient temperature is also very impressive (0.54). Unlike 1, which becomes weakly emissive in PMMA, compound 4 retains a moderate emission efficiency (0.16) in doped PMMA films. Furthermore, consistent with the TD-DFT data, the emission energy of 4 is much higher than that of 1, emitting a distinct blue−green color with λ_{max} = 500−518 nm, depending on the physical state of the sample. Compound 4 also has the longest lifetime among all the complexes. The reduced twist of the phazolyl unit relative to the ph-py unit in 1 may be responsible for the much smaller nonradiative decay rate constant, knr, and the higher emission quantum efficiency of 4.

The trigonal planar compound 5 has very low emission quantum efficiency at ambient temperature and 77 K. Its emission spectra undergo a significant and progressively blue shift from powder, crystals, to PMMA film and the frozen solution with a 90 nm of λ_{max} difference between the powder sample and the frozen solution. Intramolecular interactions and the weak pyridyl−Cu π interactions in 5 may be responsible for its low phosphorescent efficiency. The luminescent properties of 6 resemble those of 5 with nearly a 90 nm blue shift of the emission λmax from powder to the frozen solution and consistently low emission quantum efficiency. Again, the highly twisted and distorted structure of 6 may be responsible for its low emission efficiency. With the phosphorescent energy of the copper complexes in the frozen solution at 77 K as the intrinsic property of each molecule, the emission energy follows the order of 4 > 3 ≈ 5 > 1 ≈ 6 > 2, which agrees with the TD-DFT calculated trend of the vertical excitation energy to T1.

Conclusions

A series of new phenyl-bridged PΛN, PΛNΛP, and NΛPΛP ligands, as well as the corresponding copper (I) complexes, were successfully synthesized and fully characterized. The simple and solvent-free mechanochemical method was applied successfully in the preparation of some of the new complexes in high yields. X-ray crystallographic analysis revealed unusual distorted trigonal planar coordination geometry for 5 and approximately tetrahedral geometries for other complexes. The new Cu(I) complexes are stable in the solutions, which can be attributed to the chelation by the bidentate or tridentate ligands. All complexes investigated in this work are phosphorescent in the solid state or in doped PMMA films with emission colors covering the entire visible region from blue to deep red. Experimental and computational work demonstrated that the phosphorescent properties of the Cu(I) compounds are highly dependent on the N-heteroaryl ring, the geometry of the ligands/the complexes, and the state of and the environment around the complex.

EXPERIMENTAL SECTION

General Information. Air- and water-sensitive reactions were carried out in oven-dried glassware under a nitrogen or argon atmosphere. Solvents were dried using standard procedures prior to use. All reagents are of analytical grade and were used without further purification. Thin-layer chromatography was carried out on silica gel plates (silica gel 60, F254, Merck) with detection by 254 or 365 nm UV light. Purification was performed with preparative chromatography using normal-phase silica gel (silica gel 60, 230−400 mesh) or basic alumina. 1 H NMR (400 MHz), 13C NMR (101 MHz), and 31P NMR (162 MHz) spectra were recorded on a Bruker Avance-400 spectrometer. Chemical shifts are reported as δ values (ppm) relative to SiMe4 for 1 H NMR (internal standard) and 85% aqueous H3PO4 for 31P NMR (external standard). UV−vis spectra were recorded on an Agilent Cary 300 scan UV−vis absorption spectrophotometer. Excitation and emission spectra, time-resolved phosphorescence spectra, and luminescent decay lifetimes were recorded on Edinburgh Instruments FLS980 spectrophotometer, equipped with a xenon flash lamp. All solutions for photophysical data measurements were degassed under a nitrogen atmosphere. The absolute photoluminescence quantum yields were measured on a Hamamatsu QY C11347-11 spectrometer. High-resolution mass spectra (HRMS) were obtained from an Agilent Q-TOF 6520 LC-MS spectrometer. Elemental analysis was performed on a EuroVector EA3000 instrument (EuroVector, SpA). Precursors 2-(2-fluorophenyl)- pyridine,30 2,6-bis(2-fluorophenyl)pyridine,31 2-(2-bromophenyl)- pyridine,36 and ligand 2-(2-(diphenylphosphanyl)phenyl)pyridine (L1) 29 were prepared according to previously reported procedures.

Synthesis of P^N Ligands.

4-(2-Fluorophenyl)-1-methyl-1H1, 2, 3-triazole. A mixture of 1-ethynyl-2-fluorobenzene (0.732 g, 6.1 mmol), sodium azide (0.397 g, 6.1 mmol), iodomethane (0.866 g, 6.1 mmol), and CuI (0.012 g, 0.06 mmol) in 10 mL of water was heated to 65 °C for 17 h. After being cooled to room temperature, CH_2Cl_2 (40 mL) was added. The organic layer was separated and washed with water twice, dried over anhydrous Na_2SO_4, and evaporated under vacuum. The crude product was further purified by column chromatography on silica gel using petroleum ether/AcOEt (10:1) as eluent to obtain the product as white powder. Yield: 0.73 g (68%). 1 H NMR (400 MHz, $CDCl_3$): δ 8.28 (td, J = 7.6, 1.9 Hz, 1H), 7.91 (d, J = 3.7 Hz, 1H), 7.39−7.18 (m, 2H), 7.14−7.09 (m, 1H), 4.14 (s, 3H). 13C{H} NMR (100 MHz, $CDCl_3$): δ 159.22 (d, J = 247.6 Hz), 141.39, 129.29 (d, J = 8.5 Hz), 127.80 (d, J = 3.6 Hz), 124.62 (d, J = 3.3 Hz), 123.73 (d, J = 12.6 Hz), 118.56 (d, J = 12.9 Hz), 115.65 (d, J = 21.7 Hz), 36.74.

4-(2-(Diphenylphosphanyl) phenyl)-1-methyl-1H-1,2,3-triazole (L2). To solution of 4-(2-fluorophenyl)-1-methyl-1H-1,2,3-triazole (0.481 g, 2.72 mmol) and 18-crown-6 (0.934 g, 3.53 mmol) in THF (25 mL) was slowly added a 0.5 M solution of potassium diphenylphosphide (6.6 mL, 3.50 mmol) in THF at 0 °C. The mixture was stirred at room temperature for 24 h, after which water (10 mL) was added, and it was concentrated in vacuum. Et_2O (60 mL) was added, and the organic phase was washed with water twice, dried over anhydrous Na_2SO_4, and evaporated under vacuum. The crude product was further purified by column chromatography on basic alumina 90 column using petroleum ether/AcOEt (8:1) as eluent to obtain the product as white solid. Yield: 0.66 g (71%). 1 H NMR (400 MHz, $CDCl_3$): δ 8.03 (ddd, J = 7.8, 4.1, 1.1 Hz, 1H), 7.65 (d, J = 1.8 Hz, 1H), 7.49 (td, J = 7.6, 1.3 Hz, 1H), 7.39−7.33 (m, 6H), 7.31−7.24 (m, 5H), 7.01 (ddd, J = 7.7, 4.4, 1.1 Hz, 1H), 4.06 (s, 3H). 31P{H} NMR (162 MHz, $CDCl_3$): δ −11.10. HRMS (ESI) calcd for $C_{21}H_{18}N_3P$ [M + H^+] 344.1311; found 344.1331.

2, 6-Bis (2-(diphenyl-phosphanyl)-phenyl) pyridine (L3). To solution of 2,6-bis(2-fluorophenyl)pyridine (152 mg, 0.57 mmol) and 18- crown-6 (391 mg, 1.48 mmol) in THF (15 mL) was slowly added a 0.5 M solution of potassium diphenylphosphide (2.7 mL, 1.37 mmol) in THF at 0 °C. The mixture was stirred at room temperature for 48 h, after which water (10 mL) was added, and it was concentrated in vacuum. Et_2O (50 mL) was added, and the organic phase was washed with water twice, dried over anhydrous Na_2SO_4, and evaporated under vacuum. The crude product was further purified by column chromatography on basic alumina 90 column using petroleum ether to petroleum ether/EtOAc (20:1) as eluent to obtain the product as white solid. Yield: 0.27 g (80%). 1 H NMR (700 MHz, CD_2Cl_2): δ 7.55 (t, J = 7.7 Hz, 1H), 7.43 (ddd, J = 7.6, 4.3, 1.2 Hz, 2H), 7.34−7.24 (m, 18H), 7.23−7.18 (m, 8H), 7.06 (ddd, J = 7.7, 3.9, 1.1 Hz, 2H). 31P {H} NMR (162 MHz, $CDCl_3$): δ −11.33. HRMS (ESI) calcd for $C_{41}H_{31}NP_2$ [M + H+] 600.2004; found 600.2045.

2,2′-((Phenylphosphanediyl)bis(2,1-phenylene))dipyridine (L4). Under an argon atmosphere, n-BuLi (2.79 mL, 2.5 M in hexane) was added dropwise to a solution of 2-(2-bromophenyl)pyridine (1.635 g, 6.99 mmol) in THF (60 mL) at −78 °C. The resulting mixture was stirred for 1 hr at −78 °C. Then phenylphosphine dichloride (0.619 g, 3.46 mmol) was added in one portion. After being stirred for another 1 h, the reaction mixture was allowed to warm to room temperature and stirred overnight. Subsequently, water (10 mL) was added, and the reaction mixture was extracted with DCM (50 mL × 3). Then the combined organic solution was dried over anhydrous Na2SO4 and evaporated under vacuum, and the crude product was further purified by column chromatography on silica gel using petroleum ether/AcOEt (2:1) as eluent to obtain the product as yellow solid. Yield: 0.53 g (37%). 1 H NMR (400 MHz, $CDCl_3$): δ 8.45−8.43 (m, 2H), 7.55−7.52 (m, 2H), 7.45 (td, J = 7.6, 1.6 Hz, 2H), 7.36 (td, J = 7.5, 1.3 Hz, 2H), 7.25−7.22 (m, 9H), 7.17−7.14 (m, 2H), 7.04 (ddd, J = 7.5, 4.9, 1.0 Hz, 2H). 13C{H} NMR (100 MHz, $CDCl_3$): δ 158.65 (d, J = 3.3 Hz), 148.63, 145.37 (d, J = 25.3 Hz), 138.81 (d, J = 13.9 Hz), 136.84 (d, J = 17.0 Hz), 135.26, 134.80, 134.15 (d, J = 20.5 Hz), 129.52 (d, J = 4.7 Hz), 128.46, 128.27 (d, J = 6.6 Hz), 128.13, 128.12 (d, J = 3.4 Hz), 123.99 (d, J = 5.9 Hz), 121.56. 31P{H} NMR (162 MHz, CDCl3): δ −16.87. HRMS (ESI) calcd for $C_{28}H_{21}N_2P$ [M + H+] 417.1515; found 417.1532.

Synthesis of Copper Complexes. [(2-(2-(Diphenylphosphanyl)- phenyl)pyridine)(PPh_3)CuI] (1). To a dichloromethane solution (15 mL) of L1 (170 mg, 0.5 mmol) were added CuI (95 mg, 0.5 mmol) and PPh_3 (131 mg, 0.5 mmol). The mixture was stirred at room temperature for 2 h, and then solvent was removed under reduced pressure. The yellow powder was collected by filtration and washed with diethyl ether and dried under vacuum. The crude product was recrystallized from CH_2Cl_2 to obtain

complex 1 as yellow crystals. Yield: 317 mg (80%). 1 H NMR (400 MHz, $CDCl_3$): δ 9.50 (s, 1H), 7.57 (td, J = 7.8, 1.7 Hz, 1H), 7.48 (td, J = 7.6, 1.2 Hz, 1H), 7.44−7.22 (m, 18H), 7.21−7.12 (m, 10H), 7.10−7.04 (m, 1H), 6.82 (t, J = 7.6 Hz, 1H). 31P{H} NMR (162 MHz, CDCl3): δ −1.39, −13.85. Anal. Calcd for $C_{41}H_{33}CuINP_2$: C, 62.17; H, 4.20; N, 1.77. Found: C, 62.02; H, 4.16; N, 1.85.

[(2-(2-(Diphenyl phosphanyl) phenyl) pyridine)2Cu$_2$I$_2$] (2). To a dichloromethane solution (15 mL) of L1 (212 mg, 0.63 mmol) was added CuI (119 mg, 0.63 mmol). The mixture was stirred at room temperature for 2 h, and then solvent was removed under reduced pressure. The yellow powder was collected by filtration and then washed with diethyl ether. The crude product was recrystallized from CH_2Cl_2 and petroleum ether to obtain complex 2 as yellow crystals. Yield: 313 mg (85%). 1 H NMR (400 MHz, $CDCl_3$): δ 9.09 (d, J = 4.9 Hz, 2H), 7.58−7.48 (m, 9H), 7.48−7.39 (m, 4H), 7.32−7.22 (m, 7H), 7.21−7.16 (m, 10H), 6.98 (t, J = 6.6 Hz, 2H), 6.89 (t, J = 8.0 Hz, 2H). 31P{H} NMR (162 MHz, $CDCl_3$): δ −13.94. Anal. Calcd for $C_{46}H_{36}Cu_2I_2N_2P_2$: C, 58.84; H, 4.18; N, 5.28. Found: C, 58.43; H, 3.82; N, 5.37.

[(2,6-Bis(2-(diphenylphosphanyl)phenyl)pyridine)2Cu·BF$_4$] (3). In the glovebox, $Cu(CH_3CN)_4 \cdot BF_4$ (133 mg, 0.42 mmol) and L1 (287 mg, 0.82 mmol) were dissolved in THF (10 mL), and the mixture was stirred for 10 h. After addition of diethyl ether (20 mL), the reaction solution was stirred for an additional 0.5 h. The obtained yellow precipitates were collected by filtration, washed with diethyl ether, and dried under vacuum to obtain complex 3 as yellow powder. Yield: 283 mg (81%). 1 H NMR (400 MHz, $CDCl_3$): δ 8.20 (d, J = 5.4 Hz, 2H), 7.78 (td, J = 7.8, 1.7 Hz, 2H), 7.71−7.62 (m, 4H), 7.45−7.34 (m, 8H), 7.30−7.12 (m, 18H), 6.91−6.84 (m, 2H). 31P {H} NMR (162 MHz, $CDCl_3$): δ −4.68. Anal. Calcd for $C_{46}H_{36}BCuF_4N_2P_2$: C, 66.64; H, 4.38; N, 3.38. Found: C, 66.50; H, 4.54; N, 3.54.

[(4-(2-(Diphenylphosphanyl)phenyl)-1-methyl-1H-1,2,3-triazole)- (PPh$_3$)CuI] (4). To a dichloromethane solution (15 mL) of L4 (159 mg, 0.46 mmol) were added CuI (88 mg, 0.46 mmol) and PPh_3 (121 mg, 0.46 mmol). The mixture was stirred at room temperature for 2 h and then evaporated under reduced pressure. The white powder was collected by filtration and then washed with diethyl ether and CH2Cl2 and dried under vacuum to obtain complex 3 as white powder. Yield: 340 mg (92%). 1 H NMR (700 MHz, CD_2Cl_2): δ 7.75 (s, 1H), 7.66− 7.40 (m, 9H), 7.39−7.07 (m, 19H), 7.01 (s, 1H), 3.96 (s, 3H). 31P{H} NMR (283 MHz, CD_2Cl_2): δ −2.59, −12.35. Anal. Calcd for $C_{39}H_{33}CuIN_3P_2$: C, 52.14; H, 3.42; N, 2.64. Found: C, 51.98; H, 3.56; N, 2.83.

[(2,6-Bis(2-(diphenylphosphanyl) phenyl) pyridine)CuI] (5). To a dichloromethane solution (15 mL) of L3 (220 mg, 0.37 mmol) was added CuI (70 mg, 0.37 mmol). The mixture was stirred at room temperature for 6 h and then evaporated under reduced pressure. The crude product was recrystallized from CH_2Cl_2 and petroleum ether to obtain complex 5 as pale-yellow crystals. Yield: 232 mg (80%). 1 H NMR (400 MHz, CDCl3): 7.53−7.42 (m, 9H), 7.40−7.27 (m, 10H), 7.23−7.19 (m, 8H), 7.17−7.08 (m, 4H). 31P{H} NMR (162 MHz, $CDCl_3$): δ −6.79. Anal. Calcd for $C_{41}H_{31}CuINP_2$: C, 62.33; H, 3.95; N, 1.77 Found: C, 62.77; H, 4.20; N, 1.89. [(2,2′-((Phenylphosphanediyl)bis(2,1-phenylene))dipyridine)CuI] (6). To a THF solution (15 mL) of ligand L4 (120 mg, 0.29 mmol) was added CuI (55 mg, 0.29 mmol). The mixture was stirred at room temperature for 10 h and the solvent removed under reduced pressure. The red powder was collected by filtration and then washed with THF and dried under vacuum. Yield: 160 mg (91%). 1 H NMR (400 MHz, CDCl3): δ 9.04 (d, J = 4.6 Hz, 2H), 7.62 (td, J = 7.8, 1.5 Hz, 2H), 7.56−7.48 (m, 2H), 7.45−7.30 (m, 7H), 7.24−7.11 (m, 6H), 7.07 (t, J = 7.8 Hz, 2H). 31P{H} NMR (162 MHz, CDCl3): δ −19.56. Anal. Calcd for C28H21CuIN2P: C, 55.41; H, 3.49; N, 4.62 Found: C, 55.54; H, 3.90; N, 4.65.

Solid State Grinding Synthesis. *Complexes* 1: The mixture of CuI (19 mg, 0.1 mmol), Ph_3P (26 mg, 0.1 mmol), ligand L1 (34 mg, 0.1 mmol), and two drops of CH3CN was manually ground in a mortar

for 3 min. The obtained yellow powder was washed with diethyl ether and CH_2Cl_2/petroleum ether (2:1) and dried under vacuum. Complex 1 was obtained as yellow powder in a yield of 63 mg (84%).
Complexes 2: The mixture of CuI (19 mg, 0.1 mmol), ligand L1 (34 mg, 0.1 mmol), and two drops of CH_3CN was manually ground in a mortar for 3 min. The obtained yellow powder was washed with diethyl ether and CH_2Cl_2 and dried under vacuum. Complex 2 was obtained as yellow powder in a yield of 47 mg (89%).
Complexes 4: The mixture of CuI (19 mg, 0.1 mmol), Ph3P (26 mg, 0.1 mmol), ligand L4 (34 mg, 0.1 mmol), and two drops of CH3CN was manually ground in a mortar for 3 min. The obtained white powder was washed with CH2Cl2 and dried under vacuum. Complex 4 was obtained as white powder in a yield of 71 mg (90%).
X-ray Crystallography. Single crystals were obtained by means of a solvent diffusion method at room temperature. Thereinto, the single crystals of compounds 1, 2, 3, and 5 were grown from chloroform, crystal 4 was from dichloromethane, and crystal 6 from THF. Single crystal structure determinations were performed on a Bruker D8- Venture diffractometer with Mo target (λ = 0.71073 Å). Data were processed on a PC with the aid of the Bruker SHELXTL software package and corrected for absorption effects. All non-hydrogen atoms were refined anisotropically. The positions of hydrogen atoms were calculated and refined isotropically. The details of crystal data, collection parameters, and results of analyses are provided in the Supporting Information. The crystal data of 1, 2, 3, 4, 5, and 6 have been deposited to the Cambridge Crystallographic Data Center with deposition numbers of CCDC 1492171, 1492178, 1492173, 1492172, 1492174, and 1494044, respectively.
Theoretical Calculations. The DFT calculations were performed using Gaussian0937 software package. The ground-state geometries were fully optimized at the Becke three-parameter hybrid exchange and the Lee−Yang−Parr correlation functional (B3LYP)[38–40] level using the LanL2DZ41−44 basis set for Cu and I atoms and 6- 31G(d)45,46 basis set for all other atoms. Stationary points were further characterized by frequency analyses. TD-DFT calculations were performed to compute both singlet and triplet vertical excitation energies and oscillator strengths in the gas phase.

Table 1. Important Bond lengths and Angles of the Cu(I) Complexes bond lengths (Å) bond angles (deg)

	bond lengths (Å)		bond angles (deg)	
1	Cu(1)−P(1)	2.2666(9)	N(1)−Cu(1)−P(1)	88.54(7)
	Cu(1)−P(2)	2.2509(8)	P(1)−Cu(1)−P(2)	126.53(3)
	Cu(1)−N(1)	2.155(2)	N(1)−Cu(1)−I(1)	104.90(7)
	Cu(1)−I(1)	2.6564(4)	N(1)−Cu(1)−P(2)	114.42(7)
			P(1)−Cu(1)−I(1)	112.12(2)
			P(2)−Cu(1)−P(1)	107.46(3)
2	Cu(1)−P(1)	2.2337 (5)	N(1)−Cu(1)−P(1)	86.04(4)
	Cu(1)−N(1)	2.158(2)	P(1)−Cu(1)−I(1)	120.82(2)
	Cu(1)−I(1)	2.6027(3)	P(1)−Cu(1)−I(1′)	111.79(2)
	Cu(1)−I(1′)	2.6407(4)	N(1)−Cu(1)−I(1)	110.18(4)
	Cu(1)···Cu(1′)	2.7989(5)	N(1)−Cu(1)−I(1′)	107.91(4)
			I(1)−Cu(1)−I(1′)	115.48(1)
3	Cu(1)−P(1)	2.2406(7)	N(1)−Cu(1)−N(2)	106.50(9)
	Cu(1)−P(2)	2.2350(7)	P(1)−Cu(1)−P(2)	135.54(3)
	Cu(1)−N(1)	2.074(2)	P(1)−Cu(1)−N(1)	89.83(6)
	Cu(1)−N(2)	2.141(2)	P(1)−Cu(1)−N(2)	113.40(6)
			P(2)−Cu(1)−N(1)	123.76(6)
			P(2)−Cu(1)−N(2)	86.26(6)
4	Cu(1)−P(1)	2.263(1)	P(1)−Cu(1)−N(2)	89.8(1)
	Cu(1)−P(2)	2.240(1)	P(1)−Cu(1)−P(2)	127.41(4)
	Cu(1)−N(2)	2.042(3)	P(1)−Cu(1)−I(1)	106.54(3)
	Cu(1)−I(1)	2.6597(5)	P(2)−Cu(1)−N(2)	116.1(1)
			P(2)−Cu(1)−I(1)	108.02(3)
			N(2)−Cu(1)−I(1)	106.58(9)
5	Cu(1)−P(1)	2.2510(6)	P(1)−Cu(1)−P(2)	123.90(2)
	Cu(1)−P(2)	2.2150(6)	P(1)−Cu(1)−I(1)	113.79(2)
	Cu(1)−I(1)	2.5259(3)	P(2)−Cu(1)−I(1)	122.31(2)
	Cu(1)···N(1)	2.626(1)		
6	Cu(1)−P(1)	2.183(1)	P(1)−Cu(1)−N(1)	90.27(9)
	Cu(1)−N(1)	2.129(3)	P(1)−Cu(1)−N(2)	96.79(9)
	Cu(1)−N(2)	2.138(3)	N(1)−Cu(1)−N(2)	94.6(1)
	Cu(1)−I(1)	2.519(1)	P(1)−Cu(1)−I(1)	138.72(3)
			N(1)−Cu(1)−I(1)	115.35(8)
			N(2)−Cu(1)−I(1)	111.70(8)

Table 2. Phosphorescent Data of Copper Complexes 1−6

	λ_{max} (nm)	Φ_{PL}	τ_{av}[a] (μs)	k_r[b] (10^4 s^{-1})	k_{nr}[c] (104 s^{-1})	λ_{max} (nm)	Φ_{PL}	τ_{av}[a] (μs)	k_r[b] (10^4 s^{-1})	k_{nr}[c] (10^4 s^{-1})
Complex	**1**					**2**				
Powder[d]	601	0.15	8.3	1.8	10.3	649	0.02	9.0	0.22	10.8
Crystal [d]	581	0.33	11.0	3.0	6.1	637	0.02	9.5	0.21	10.3
Film[d]	606	0.03	7.2	0.42	13.4	617	0.02	5.7	0.35	17.2
Solution [e]	594	0.38	29.0	1.3	2.1	634	0.01	16.1	0.06	6.1
Complex	**3**					**4**				
Powder[d]	616	0.01	9.0	0.11	11.0	504	0.54	29.9	1.80	1.5
Crystal [d]	606	0.01	7.8	0.13	12.9	504	0.27	36.1	0.75	2.0
Film [d]	589	0.02	8.0	0.25	12.3	518	0.16	19.1	0.84	4.4

Solution [e]	571	0.01	63.6	0.02	1.56	500	0.97	177	0.55	0.02
Complex	**5**					**6**				
Powder[d]	656	0.01	11.4	0.09	8.7	684	0.01	9.6	0.10	10.3
Crystal [d]	626	0.01	8.8	0.11	11.3	677	0.01	10.8	0.09	9.2
Film[d]	600	0.01	9.3	0.11	10.9	588	0.01	6.9	0.15	14.4
Solution [e]	567	0.01	148.2	0.01	0.67	590	0.01	67.0	0.01	1.5

[a] Average lifetime (τ_{av}) is calculated by the equation $\tau_{av} = \Sigma A_i\tau_i^2/\Sigma A_i\tau_i$, where A_i is the pre-exponential for lifetime τ_i. The estimated standard deviation for τ_{av} is 2−10%. [b] Radiative rate constants (k_r) were estimated from the equation $k_r = \Phi/\tau av$. [c] Nonradiative rate constants (k_{nr}) were estimated from the equation $k_{nr} = k_r(1 - \Phi)/\Phi$. [d] The data for neat powder, crystals, and PMMA films doped with 5 wt % of the Cu(I) compound were recorded at room temperature.
[e]Glassy solution recorded in 2-Me-THF at 77 K.

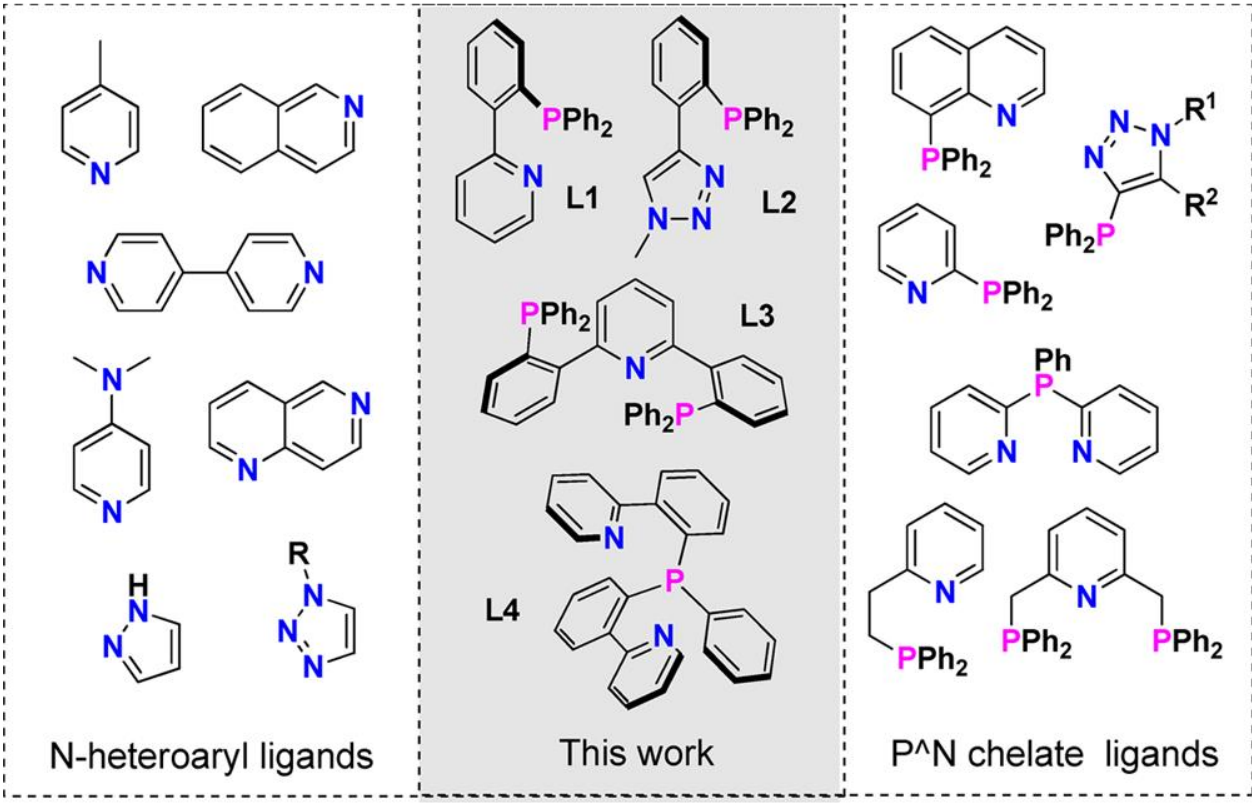

Chart 1. Examples of Commonly Used N-Heteroaryl Ligands and Previously Reported PΛN Chelate Ligands for Cu(I) Compounds and the Ligands Investigated in This Work

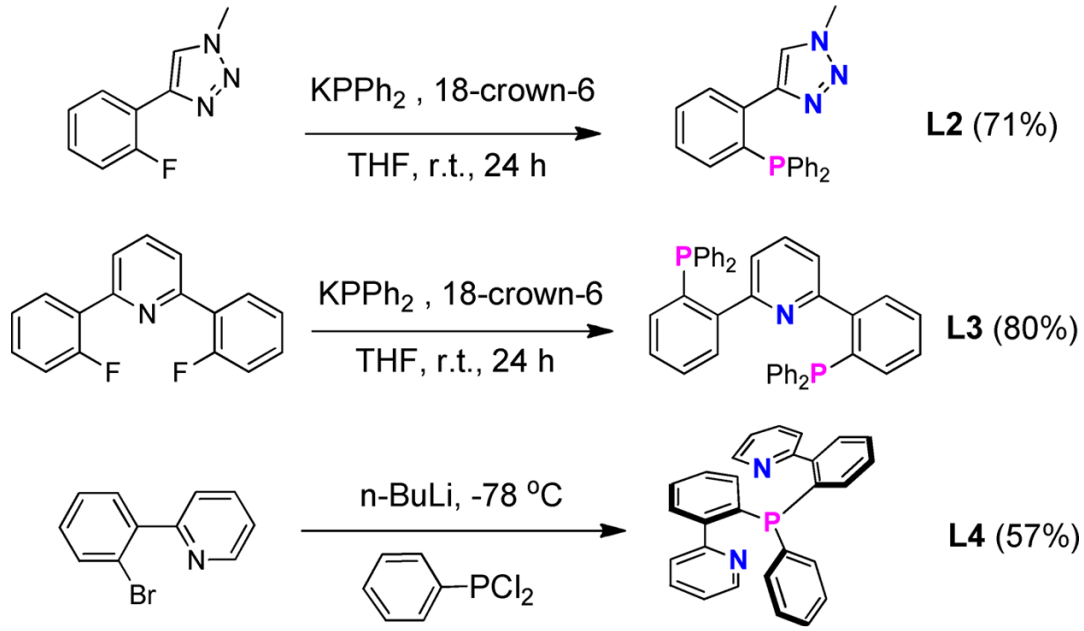

Scheme 1. Synthetic Procedures for Ligands L2, L3, and L4

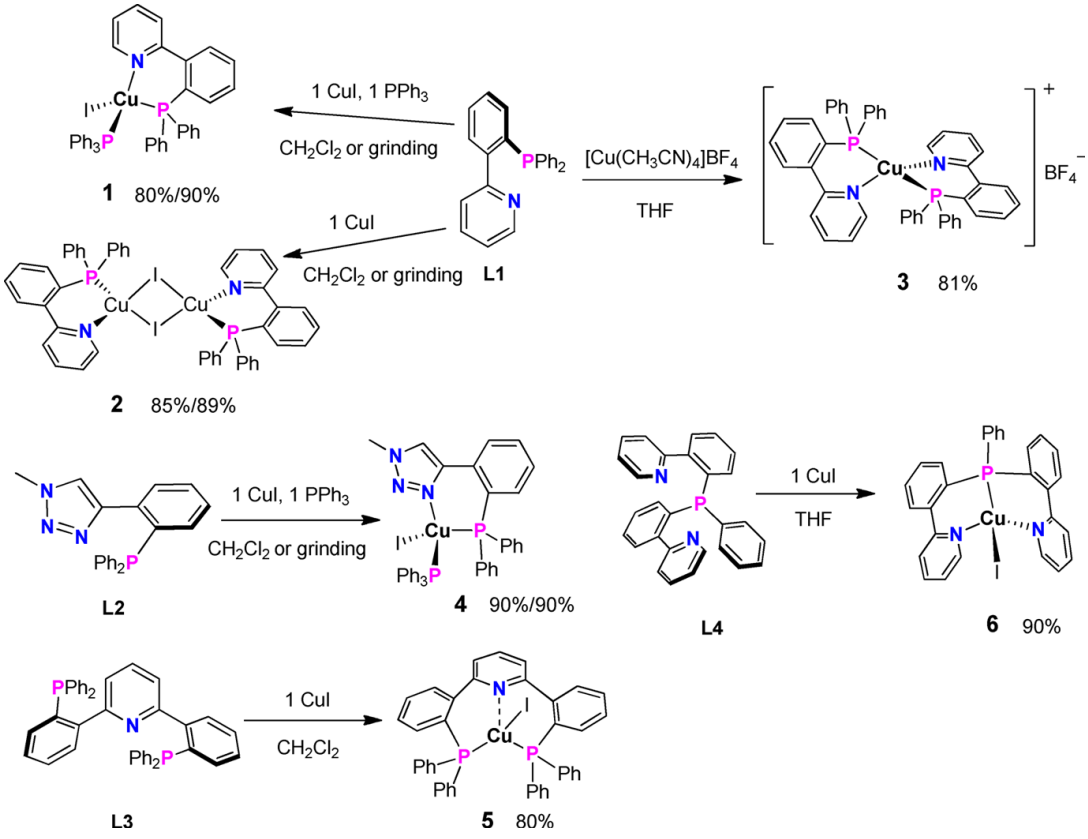

Scheme 2. Synthetic Procedures for the Cu (I) Complexes [a]

[a] The second yields for compounds 1, 2, and 4 are for the solid-state grinding procedure.

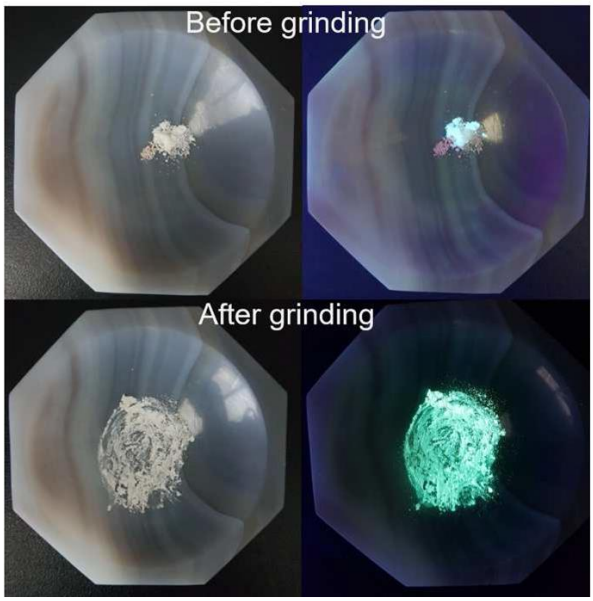

Figure 1. Photographs showing the three-component reactant mixture for compound 4 under ambient light (left) and UV light (right) before (top) and after grinding (bottom). Ligand L2 emits a weak blue color with λ_{em} = 460 nm in the solid state, which is distinctly different from the blue−green emission color of 4 (λ_{em} = 504 nm)

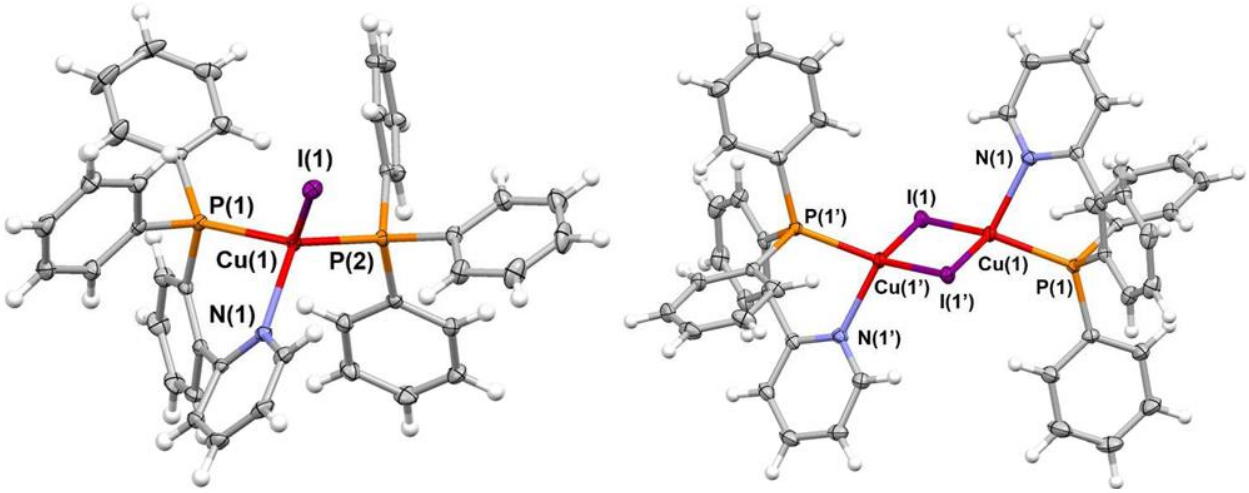

Figure 2. Crystal structures of 1 (left) and 2 (right).

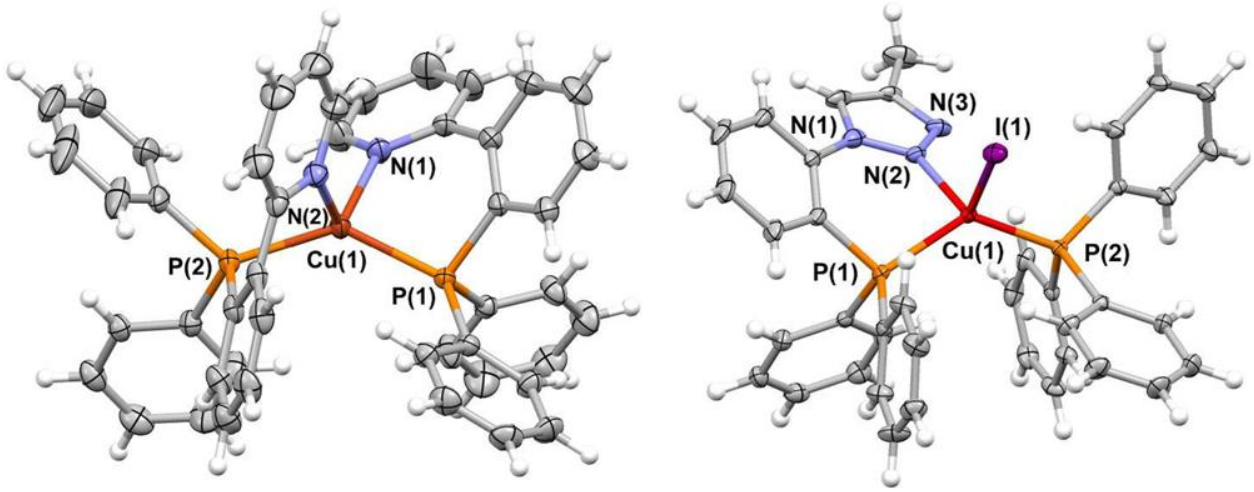

Figure 3. Crystal structures of 3 (left) and 4 (right).

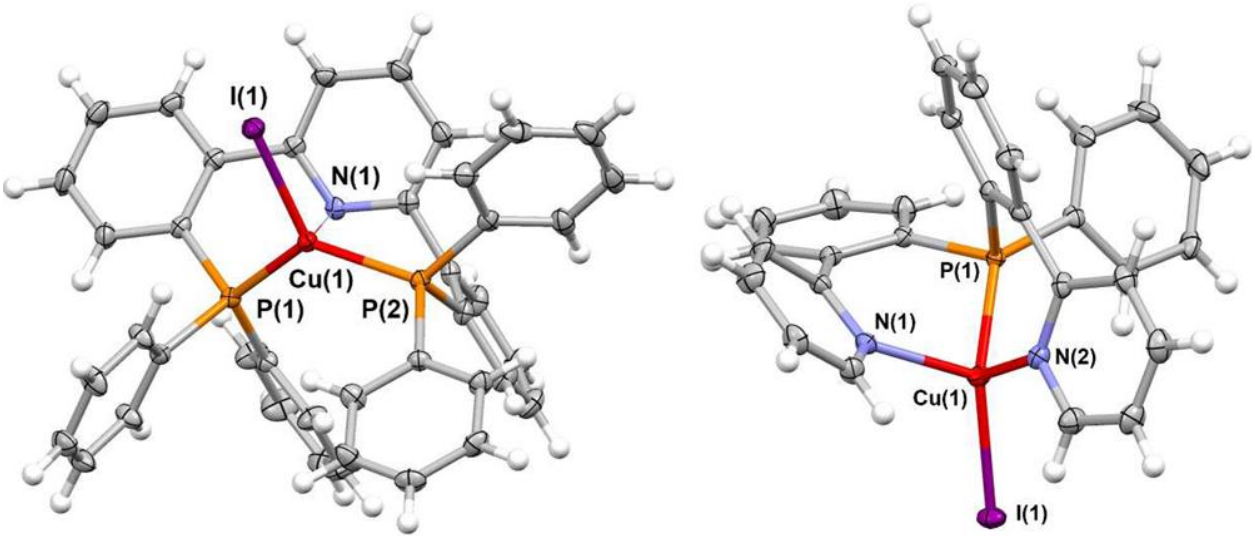

Figure 4. Crystal structures of 5 (left) and 6 (right).

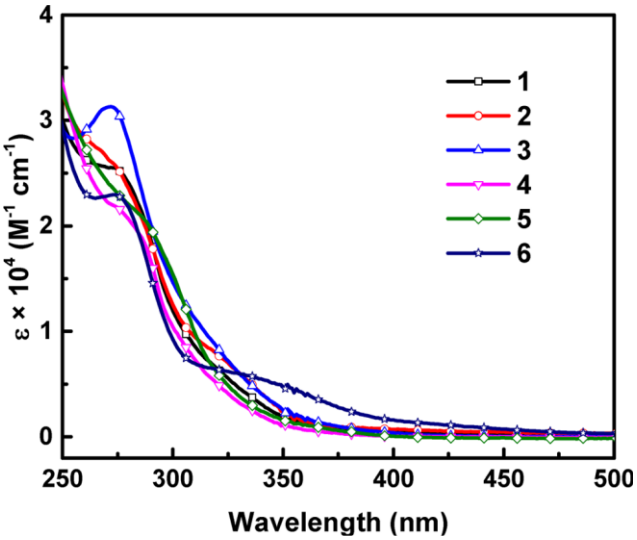

Figure 5. UV−vis absorption spectra of compounds 1−6 in in CH_2Cl_2 at room

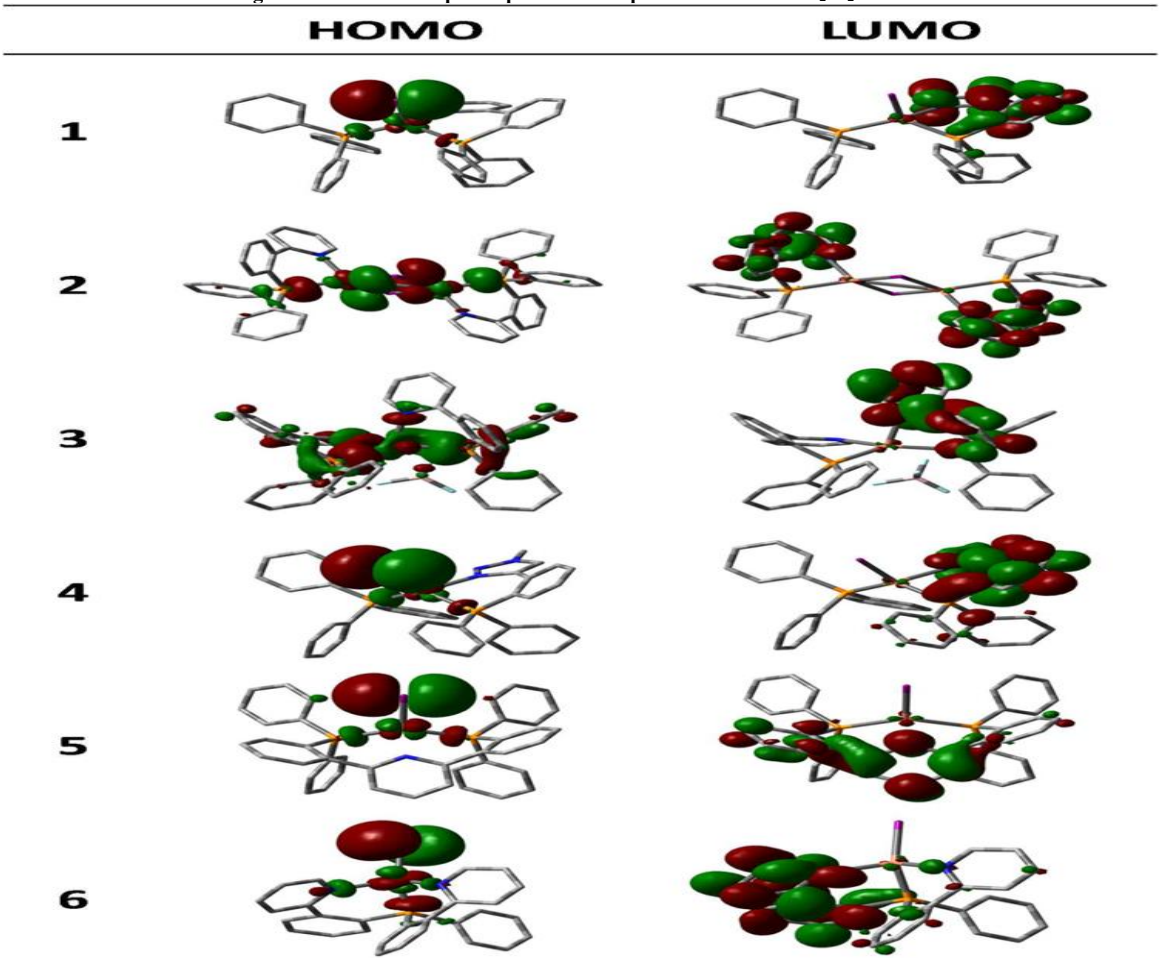

Figure 6. HOMO and LUMO diagrams for compounds 1−6.

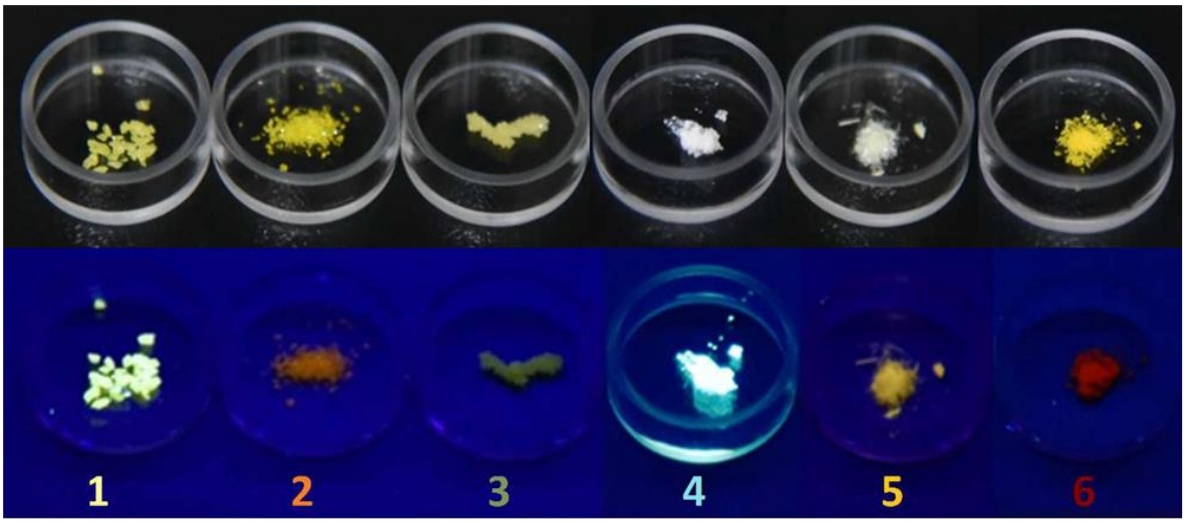

Figure 7. Photograph showing the colors of compounds 1−6 in the crystalline state under ambient light (top) and UV light (bottom).

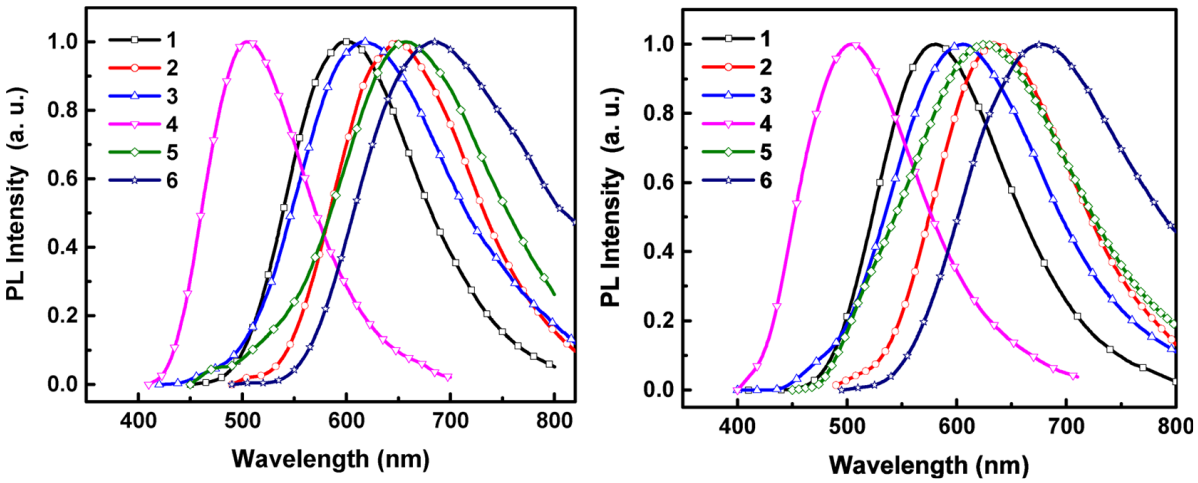

Figure 8. Normalized emission spectra of compounds 1−6 as powders (left) and as crystals (right) at 298 K.

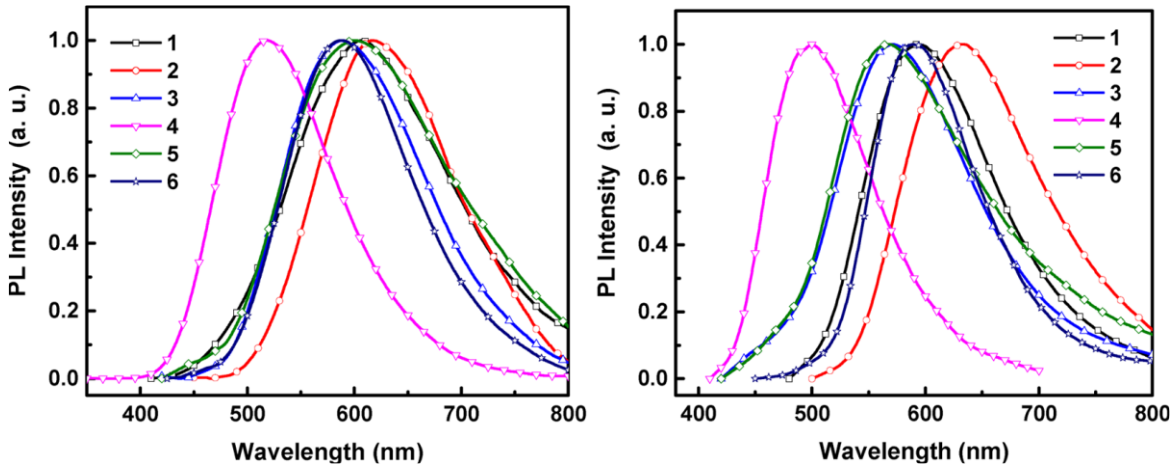

Figure 9. Normalized emission spectra of compounds 1−6 doped PMMA film (5%) at 298 K (left) and in 2-Me-THF solution at 77 K (right).

References:

1). Volz, D.; Chen, Y.; Wallesch, M.; Liu, R.; Fléchon, C.; Zink, D. M.; Friedrichs, J.; Flügge, H.; Steininger, R.; Göttlicher, J.; Heske, C.; Weinhardt, L.; Bräse, S.; So, F.; Baumann, T. Adv. Mater. 2015, 27, 2538−2543.

2). Hofbeck, T.; Monkowius, U.; Yersin, H. J. Am. Chem. Soc. 2015, 137, 399−404.

3). Zink, D. M.; Volz, D.; Baumann, T.; Mydlak, M.; Flügge, H.; Friedrichs, J.; Nieger, M.; Bräse, S. Chem. Mater. 2013, 25, 4471−4486.

4). Zhang, Q.; Zhou, Q.; Cheng, Y.; Wang, L.; Ma, D.; Jing, X.; Wang, F. Adv. Mater. 2004, 16, 432−436.

5). Sun, Y.; Lemaur, V.; Beltrán, J. I.; Cornil, J.; Huang, J.; Zhu, J.; Wang, Y.; Fröhlich, R.; Wang, H.; Jiang, L.; Zou, G. Inorg. Chem. 2016, 55, 5845−5852.

6). Luo, S.-P.; Mejía, E.; Friedrich, A.; Pazidis, A.; Junge, H.; Surkus, A.-E.; Jackstell, R.; Denurra, S.; Gladiali, S.; Lochbrunner, S.; Beller, M. Angew. Chem. 2013, 125, 437−441.

7). Wang, B.; Shelar, D. P.; Han, X.-Z.; Li, T.-T.; Guan, X.; Lu, W.; Liu, K.; Chen, Y.; Fu, W.-F.; Che, C.-M. Chem. - Eur. J. 2015, 21, 1184−1190.

8). Windisch, J.; Orazietti, M.; Hamm, P.; Alberto, R.; Probst, B. ChemSusChem 2016, 9, 1719−1726.

9). Medina-Rodriguez, S.; Orriach-Fernandez, F. J.; Poole, C.; Kumar, P.; de la Torre-Vega, A.; Fernandez-Sanchez, J. F.; Baranoff, E.; Fernandez-Gutierrez, A. Chem. Commun. 2015, 51, 11401−11404.

10). Xin, X.-L.; Chen, M.; Ai, Y.-b.; Yang, F.-l.; Li, X.-L.; Li, F. Inorg. Chem. 2014, 53, 2922−2931.

11). Brauchli, S. Y.; Bozic-Weber, B.; Constable, E. C.; Hostettler, N.; Housecroft, C. E.; Zampese, J. A. RSC Adv. 2014, 4, 34801−34815.

12). Wills, K. A.; Mandujano-Ramirez, H. J.; Merino, G.; Mattia, D.; Hewat, T.; Robertson, N.; Oskam, G.; Jones, M. D.; Lewis, S. E.; Cameron, P. J. RSC Adv. 2013, 3, 23361−23369.

13). Bessho, T.; Constable, E. C.; Graetzel, M.; Hernandez Redondo, A.; Housecroft, C. E.; Kylberg, W.; Nazeeruddin, M. K.; Neuburger, M.; Schaffner, S. Chem. Commun. 2008, 3717−3719.

14). Ford, P. C.; Cariati, E.; Bourassa, J. Chem. Rev. 1999, 99, 3625−3648.

15). Xu, H.; Chen, R.; Sun, Q.; Lai, W.; Su, Q.; Huang, W.; Liu, X. Chem. Soc. Rev. 2014, 43, 3259−3302.

16). Dias, H. V. R.; Diyabalanage, H. V. K.; Rawashdeh-Omary, M. A.; Franzman, M. A.; Omary, M. A. J. Am. Chem. Soc. 2003, 125, 12072−12073.

17). Dias, H. V. R.; Diyabalanage, H. V. K.; Eldabaja, M. G.; Elbjeirami, O.; Rawashdeh-Omary, M. A.; Omary, M. A. J. Am. Chem. Soc. 2005, 127, 7489−7501.

18). Araki, H.; Tsuge, K.; Sasaki, Y.; Ishizaka, S.; Kitamura, N. Inorg. Chem. 2005, 44, 9667−9675.

19). Ohara, H.; Kobayashi, A.; Kato, M. Dalton Trans. 2014, 43, 17317−17323.

20). Wallesch, M.; Volz, D.; Zink, D. M.; Schepers, U.; Nieger, M.; Baumann, T.; Bräse, S. Chem. - Eur. J. 2014, 20, 6578−6590.

21). Kobayashi, A.; Hasegawa, T.; Yoshida, M.; Kato, M. Inorg. Chem. 2016, 55, 1978−1985.

22). Musina, E. I.; Shamsieva, A. V.; Strelnik, I. D.; Gerasimova, T. P.; Krivolapov, D. B.; Kolesnikov, I. E.; Grachova, E. V.; Tunik, S. P.; Bannwarth, C.; Grimme, S.; Katsyuba, S. A.; Karasik, A. A.; Sinyashin, O. G. Dalton Trans. 2016, 45, 2250−2260.

23). Zink, D. M.; Grab, T.; Baumann, T.; Nieger, M.; Barnes, E. C.; Klopper, W.; Bräse, S. Organometallics 2011, 30, 3275−3283.

24). Wei, F.; Liu, X.; Liu, Z.; Bian, Z.; Zhao, Y.; Huang, C. Cryst Eng Comm 2014, 16, 5338−5344.
25). Zink, D. M.; Bächle, M.; Baumann, T.; Nieger, M.; Kühn, M.; Wang, C.; Klopper, W.; Monkowius, U.; Hofbeck, T.; Yersin, H.; Bräse, S. Inorg. Chem. 2013, 52, 2292−2305.
26). Zink, D. M.; Baumann, T.; Friedrichs, J.; Nieger, M.; Bräse, S. Inorg. Chem. 2013, 52, 13509−13520.
27). Liu, Z.; Djurovich, P. I.; Whited, M. T.; Thompson, M. E. Inorg. Chem. 2012, 51, 230−236.
28). Volz, D.; Zink, D. M.; Bocksrocker, T.; Friedrichs, J.; Nieger, M.; Baumann, T.; Lemmer, U.; Bräse, S. Chem. Mater. 2013, 25, 3414−3426.
29). Flapper, J. K. H.; Kooijman, H.; Lutz, M.; Spek, A. L.; Van Leeuwen, P. W. N. M.; Elsevier, C. J.; Kamer, P. C. J. Organometallics 2009, 28, 1180−1192.
30). Clavier, S.; Rist, O.; Hansen, S.; Gerlach, L. O.; Hogberg, T.; Bergman, J. Org. Biomol. Chem. 2003, 1, 4248−4253.
31). Winston, M. S.; Bercaw, J. E. Organometallics 2010, 29, 6408− 6416.
32). Kobayashi, A.; Hasegawa, T.; Yoshida, M.; Kato, M. Inorg. Chem. 2016, 55, 1978−1985.
33). Zhao, S. B.; Wang, R. Y.; Wang, S. Inorg. Chem. 2006, 45, 5830− 5840.